
An in vitro study of two GAG-like marine polysaccharides incorporated into injectable hydrogels for bone and cartilage tissue engineering

E. Rederstorff^{a,b}, P. Weiss^{a,*}, S. Sourice^a, P. Pilet^a, F. Xie^a, C. Siquin^b, S. Collic-Jouault^b, J. Guicheux^a and S. Laïb^a

^a INSERM UMRS 791, University of Nantes, Laboratory of Osteo-Articular and Dental Tissue Engineering, School of Dental Surgery, 1 Place Alexis Ricordeau, 44042 Nantes cedex 1, France

^b Ifremer, Laboratory of Biotechnology and Marine Molecules, Rue de l'Île d'Yeu BP 21105, 44311 Nantes Cedex 03, France

*: Corresponding author : Tel.: +33 240 412 914; fax: +33 240 083 712
Email address: pweiss@sante.univ-nantes.fr (P. Weiss)

Abstract:

Natural polysaccharides are attractive compounds with which to build scaffolds for bone and cartilage tissue engineering. Here we tested two non-standard ones, HE800 and GY785, for the two-dimensional (2-D) and three-dimensional (3-D) culture of osteoblasts (MC3T3-E1) and chondrocytes (C28/I2). These two glycosaminoglycan-like marine exopolysaccharides were incorporated into an injectable silylated hydroxypropylmethylcellulose-based hydrogel (Si-HPMC) that has already shown its suitability for bone and cartilage tissue engineering. Results showed that, similarly to hyaluronic acid (HA) (the control), HE800 and GY785 significantly improved the mechanical properties of the Si-HPMC hydrogel and induced the attachment of MC3T3-E1 and C28/I2 cells when these were cultured on top of the scaffolds. Si-HPMC hydrogel containing 0.67% HE800 exhibited the highest compressive modulus (11 kPa) and allowed the best cell dispersion, especially of MC3T3-E1 cells. However, these cells did not survive when cultured in 3-D within hydrogels containing HE800, in contrast to C28/I2 cells. The latter proliferated in the microenvironment or concentrically depending on the nature of the hydrogel. Among all the constructs tested the Si-HPMC hydrogels containing 0.34% HE800 or 0.67% GY785 or 0.67% HA presented the most interesting features for cartilage tissue engineering applications, since they offered the highest compressive modulus (9.5–11 kPa) while supporting the proliferation of chondrocytes.

Keywords: Glycosaminoglycan, Hydrogel, Polysaccharide, Bone and Cartilage Tissue Engineering, In vitro test

1. Introduction

In bone and cartilage tissue engineering, a great number of natural polysaccharides have been widely studied due to their biodegradability, biocompatibility and capacity of mimicking the extracellular matrix while providing a temporary mechanical support (1-3). Of these polysaccharides, the most widely investigated are chitin (4), chitosan (5, 6), alginate (7, 8), cellulose derivatives (9), dextran (10), and compounds from the GAG family such as hyaluronic acid (11-13) and chondroitin sulfate (14). So far, no scaffold made of these polysaccharides or combination of them have shown an adequate combination of mechanical and biological properties. It is therefore still interesting to test new natural polysaccharides that could meet these requirements. Here we propose testing of two marine exopolysaccharides (EPSs), HE800 EPS (15, 16) and GY785 EPS (17, 18), which are a hyaluronic-like polysaccharide and a branched sulfated GAG-like polymer, respectively. Both EPSs were secreted under laboratory conditions from marine bacteria originating from deep-sea hydrothermal vents. Their large scale production is therefore convenient, low cost, reproducible, and free of non-conventional transmissible agents. HE800 is a non-sulfated linear polysaccharide with a high molecular mass (7.4×10^5 g/mol on average). Its repeating unit is a tetrasaccharide composed of two glucuronic acid units, one N-acetyl-glucosamine and one N-acetyl-galactosamine (19). GY785 is a branched nonasaccharide of high molecular mass (1.4×10^6 g/mol on average) containing 3.2% of sulfate (20). The presence of carboxylate groups on HE800 and GY785, and sulfate groups on GY785, make these polysaccharides promising candidates for promoting interactions with the cationic amino acids of proteins, such as growth factors, cytokines and cell adhesion molecules (21). Consequently they may constitute a reservoir system for proteins and play a key role in cell adhesion and cell growth (22). In a previous study, fibers of HE800 EPS were used to fill critical size defects in rat calvaria and showed strong bone healing after 3 weeks (23). In addition, HE800 and GY785, which are two hydrophilic polysaccharides of high molecular mass, should offer high viscosifying properties and strong mechanical properties similarly to hyaluronic acid (24).

In this context and as a preliminary study to further tissue engineering applications, we chose to incorporate HE800 and GY785 EPSs into a well-known cellulose-based hydrogel that has been developed in our laboratory for bone and cartilage tissue engineering. This silylated hydroxypropylmethylcellulose-based hydrogel (Si-HPMC) is injectable and auto-sets at physiological pH by a cross-link reaction involving the condensation of silanol groups (25). In previous studies, this biocompatible and biodegradable (26) hydrogel was shown to have good capacities for maintaining the growth of differentiated chondrocytes (27) and maintaining phosphate granules in bone defects (28). By adding HE800 and GY785 EPSs into the Si-HPMC hydrogel, the aim of our work was two-fold: (i) to assess the mechanical properties of the Si-HPMC hydrogel supplemented with HE800 and GY785 EPSs, and (ii) to evaluate the ability of the Si-HPMC hydrogels supplemented with HE800 or GY785 EPSs to support the viability, attachment and/or proliferation of osteoblasts and chondrocytes cultured in two and three dimensions. Hyaluronic acid (HA) was chosen as a positive control for the addition of HE800 or GY785 within Si-HPMC hydrogel. Hydrogel made from the Si-HPMC polymer only was used as a reference for all the new scaffolds. We evaluated the effects of the addition of a GAG-like polysaccharide (HE800, GY785 or HA) on the physical, chemical and bioactive properties of the Si-HPMC hydrogel using osteoblasts (MC3T3-E1) and chondrocytes (C28/I2). Various constructs were tuned and tested in order to offer an optimal environment for cells.

2. Materials and Methods

2.1. Polysaccharide origin and molecular weight determination

HE800 and GY785 exopolysaccharides were purchased from Seadev-FermenSys SAS (France). Hyaluronic acid sodium salt from *Streptococcus equi* (HA) was supplied by Sigma-Aldrich (France), and the silylated hydroxypropylmethylcellulose (Si-HPMC) was prepared as previously described (29). Briefly, a commercial hydroxypropylmethylcellulose (Methocel E4M[®], Colorcon, England) was modified by 3-glycidoxypropyltrimethoxysilane (Sigma-Aldrich, France) *via* a nucleophilic epoxide opening that occurred under heterogeneous conditions.

HE800, GY785 and HA polysaccharides were dissolved in distilled water at a concentration of 2mg/ml and filtered on a 0.45 μ m cellulose acetate syringe filter. The average molecular weight (Mw), number-average molecular weight (Mn), radius of gyration (Rg) and polydispersity ($I=Mw/Mn$) of the samples were measured using high performance size exclusion chromatography (HPSEC) combined with a multi-angle laser light scattering detector (MALLS). The system was composed of an HPLC system

Prominence Shimadzu[™], a PL aquagel-0H mixed, 8 μm (Varian) guard column (U 7.5mm* L50mm), and a PL aquagel-0H mixed (Varian) separation column (U 7.5*300mm, operating range 10^2 - 10^7 g/mol). Elution was performed at 1ml/min with 0.1M ammonium acetate containing 0.03% NaN_3 , filtrated on a 0.1 μm membrane (Durapore Membrane, PVDF, Hydrophilic type VVLP, Millipore). A differential refractive index (RI) detector (Hitachi L2490) and a multi-angle light scattering detector (Dawn Heleos II[™], Wyatt) were coupled on-line and data computed with Astra software for absolute molar mass determination.

2.2. Hydrogel formation

2.2.1. Silylated hydroxypropylmethylcellulose-based hydrogel

Si-HPMC polymer was first solubilized at 3wt% in 0.2M NaOH over 48h before being dialyzed against 0.09M NaOH using 6-8kDa dialysis tubes (SpectraPor 1, Fisher Scientific Bioblock, France). The resulting viscous solution (pH=12.6) and a 4-(2-hydroxyethyl)-1-piperazineethanesulfonic acid buffer (pH=3.6) were separately steam sterilized and then mixed with luer-lock syringes at a volume ratio of 1/0.5 before being injected into multi-well plates (Corning, VWR, France). Typically, 1ml of the hydrogel was molded per well in 24 well plates for cell culture and 2ml for compressive tests (see below). This hydrogel contained a final concentration of Si-HPMC of 2% and was noted Si-HPMC (2).

2.2.2. Si-HPMC/HE800, Si-HPMC/HA and Si-HPMC/GY785 hydrogels

HE800, HA and GY785 polysaccharides were mixed with the steam sterilized 3wt% basic solution of Si-HPMC (see § 2.2.1) at the desired concentration (1, 5, 7.5 or 10mg/ml). The resulting mixtures were left in mild rotatory stirring over one night to allow the polysaccharide to dissolve or disperse. Then, as with the preparation of the Si-HPMC hydrogel, 0.5 volume of 4-(2-hydroxyethyl)-1-piperazineethanesulfonic acid buffer (pH=3.6) was mixed with the basic solutions of polysaccharides to form hydrogels within 35 minutes maximum according to the gel point measurements (see below). For an initial concentration of 10mg of HE800 or HA or GY785 per ml of 3wt% Si-HPMC solution, the resulting hydrogels contained 2wt% of Si-HPMC and 0.67wt% of the added polysaccharide. They were noted Si-HPMC/HE800 (2/0.67), Si-HPMC/HA (2/0.67), and Si-HPMC/GY785 (2/0.67), respectively.

2.3. Hydrogel characterization

2.3.1. Osmolarity, pH and gel point measurements

Immediately (about 10 sec) after mixing the basic solutions of polymer(s) with the acid buffer, the pH of the samples (before and after hardening) was recorded on a Knick portable pH meter and the osmolarity values on an advanced micro-osmometer (model 3MO plus, Advanced Instrument Inc.) that uses the freezing point method. For gel point measurements, 3x1.5ml of each sample was injected into a rotational rheometer (RheoStress 300, Thermo Haake Co., Germany). The storage modulus G' and the loss modulus G'' were monitored as a function of time at 25°C under multi-wave oscillatory shear (1 to 30 rad/s) with a titanium plate of cone-plate geometry (60 mm diameter, 1° cone angle). The strain amplitude was fixed at 0.5 Pa, which lies in the linear viscoelastic region. The gel points are given as the time taken for the liquid ($G'' > G'$) to turn into a solid ($G' > G''$). They were determined according to a derived percolation theory (30), which says that near the gel point, $G' \sim G'' \sim \omega^n$ over a range of frequencies so G''/G' can be expressed as $\tan \delta = G''(\omega) / G'(\omega) = \tan(n\pi/2)$ (where n is the relaxation exponent). Also, at the gel point, the phase angle between stress and strain, δ , is independent of frequency but proportional to the relaxation exponent: $\delta = n\pi/2$. Consequently, all the curves of $\tan \delta$ versus time at different frequencies have a common intersection point which defines the gel point.

2.3.2. Compressive modulus measurements

6x2ml of each hydrogel, prepared as described in paragraph 2.2., were molded into 24-well plates and left for cross-linking for 15±3hours. Then, as with 2D cell culture (see paragraph 2.4.3), 0.5ml of culture medium was added per well and allowed to diffuse within the hydrogel over 48h. The resulting hydrogels were unmolded, and the diameter and height of each cylinder were measured with a calliper square. The hydrogels were then compressed to rupture on a TA.HD *plus* Texture Analyser (Stable Micro Systems Lts, England) with a cylinder load (diameter of 25mm, LAP Perspex, England) of 1g

moving at 1mm/sec to plot the force (Pa) as a function of the strain. The compressive modulus was calculated as the slope of the curve between 0% and 10% of strain.

2.3.3. Scanning electron microscopy

The hydrogels were molded into 24-well plates and allowed to crosslink over one night before being flash frozen by immersion in isopentane cooled down by liquid nitrogen. The frozen samples were immediately lyophilized and coated with carbon on a Jeol Jee-4B (Japan). The scanning electron images of the surface of the hydrogels were recorded on a Leo 1450VP microscope (Zeiss SMT, Germany) at 20 kV.

2.4. Cell culture

2.4.1. Cell lines

MC3T3-E1 and C28/I2 cells were cultured in a 5% CO₂ incubator at 37 °C in α -MEM and DMEM F-12 medium (Invitrogen corporation, France), respectively. Both culture media were supplemented with 10% of fetal bovine serum (FBS), 1% of penicillin/streptomycin and 1% of L-glutamine, which were changed every 2-3 days.

2.4.2. Cell viability in 2D and 3D cultures

MC3T3-E1 and C28/I2 cells were allowed to attach to 24-well plates at a final density of 20,000 cells per well. After 24h, the culture medium was removed and 500 μ l of each cross-linked hydrogel was added per well. The samples were incubated at 37°C for 1h before adding 1ml of culture medium. As a positive control, cells were cultured in the absence of Si-HPMC hydrogel. As a negative control, cells were cultured in the presence of actinomycin-D (5 μ g/ml), which is a transcription inhibitor. After 24, 48 or 72h of culture, the hydrogels and culture media were removed by aspiration. Trypan blue exclusion dye assays were performed to count the cells and the Methyl Tetrazolium Salt (MTS; Promega, USA) test was performed to evaluate their mitochondrial activity. For the latter, a MTS solution was added to each well for 1-3h according to the manufacturer's instructions. The optical density of formazan dye was measured on a spectrophotometer at 490nm. Each condition was tested in triplicate and the results were expressed as relative MTS activities as compared to the positive control.

For 3D culture, cell viability was quantitatively assessed by Live&Dead assays (Kit, Invitrogen, France) along with confocal image analysis. Briefly, MC3T3-E1 and C28/I2 cells were dispersed into the hydrogels within the 5 minutes following their preparation at a final concentration of one million cells per ml of hydrogel. 800 μ l of each mixture was molded into ultra-low attachment 24-well plates and incubated at 37°C for 1h to allow the hydrogels to crosslink. Afterwards, 1ml of appropriate culture medium was added per well and the samples were incubated for 48h before Live&Dead assays were performed. Actinomycin-D treatment (5 μ g/mL) was used as an internal control of cell death. In each well, the culture medium was replaced by 200 μ l of a solution containing 2.5ml of complete DMEM-F12 medium for C28/I2 cells or α -MEM for MC3T3-E1 cells supplemented with 0.25 μ l of calcein-AM and 5 μ L of ethidium homodimer-1. After 5 to 10 minutes, the dye mixture was removed and the hydrogels were intensively rinsed with some phosphate buffered saline before being observed on a confocal laser-scanning microscope (Nikon D-eclipse C1) equipped with an argon/krypton laser. For each sample, 6 random positions (x,y,z) were chosen within the hydrogel, and series of 35 images were taken from these 6 positions along the z axis in 5 μ m stages. The 210 images obtained per sample were analyzed with a quantimeter Q550 (Leica microsystem GmbH, Wetzlar, Germany). The percentages of living cells (in green) and dead cells (in red) were determined by using a customized image analysis program made in our laboratory.

2.4.3. Morphology and spatial organization of cells in 2D culture

MC3T3-E1 and C28/I2 cells were seeded on to cross-linked hydrogels containing the final concentration of HE800, HA or GY785 ranging from 0% to 0.67%. 3x300 μ l of each hydrogel were molded into ultra-low attachment 24-well plates and left at room temperature for 1h for cross-linking. 500 μ l of complete medium was added to each well and the samples were incubated at 37°C overnight before seeding the cells at a final density of 20,000 cells per well. After 48h of culture, cells were observed with an inverted optical microscope (Nikon Instruments, The Netherlands), and the number of cells that remained in the culture media was determined by trypan blue exclusion dye assays. To stain and count the cells per cluster, culture media were removed and replaced by a PBS-4% paraformaldehyde solution. The samples were fixed for 20min at 4°C and left 15min at 4°C in a PBS-

0.1% of Triton X-100 solution. The cells were then incubated with Alexafluor 488-phalloidin (A12379, Molecular probe, Invitrogen) at a dilution of 1:40 in PBS-bovine serum albumin (BSA-10mg/ml) for 1h at 37°C in the dark to stain cytoskeletal F-actin fibers in green. The samples were then rinsed with PBS- 0.05% Tween and incubated with Hoechst at 5mg/ml in deionized water for 10 min at room temperature to stain the nuclei blue. Finally, the samples were rinsed twice with deionized water and observed with a Nikon TE2000-E inverted microscope in the green and blue excitation ranges, separately. Images were overlaid using ImageJ Software. For each condition, 20 clusters were randomly selected to count the number of blue nuclei.

2.4.4. Morphology and spatial organization of cells in 3D culture

MC3T3-E1 and C28/I2 cells were cultured in 3D as described in § 2.4.2. After 5 weeks of culture, some cells were stained by Live&Dead assays (see § 2.4.2.), and some were fixed in formol over 1h and embedded into a 2% agarose solution before embedding in paraffin. Serial sections of each paraffin block (5µm thickness) were made and processed for routine histology (hematoxylin/eosin/safranin-O or alcian blue staining). Samples were observed with a Nikon TE2000-E inverted microscope.

2.5. Statistical analysis

Experiments were repeated at least three times. Data were analyzed using ANOVA with a post-hoc test (Fisher's project least significant difference). Statistical significance was set to a p value ≤ 0.05 and the results are expressed as mean \pm SEM.

3. Results

3.1. Polysaccharide characteristics and hydrogel preparation

As seen in Table 1, the physical and chemical characteristics of the selected hyaluronic acid (the positive control) match those of the HE800 EPS (the polysaccharide tested). GY785 EPS has similar features except that it contains sulfate and has a 2-fold higher average molecular weight (Mw). HE800, HA and GY785 polysaccharides were added to the Si-HPMC hydrogel by solubilizing them into the basic medium. HE800, HA and GY785 polysaccharides were completely solubilized at a concentration of 10mg/mL. At higher concentrations HE800 and GY785 were not soluble within the basic solution for which we observed a saturation of the medium contrary to HA. Si-HPMC hydrogels can be supplemented at most with 0.67% of HE800 and GY785 marine polysaccharides, which was thus used as our working concentration.

3.2. Hydrogel characterization

Si-HPMC hydrogels containing 0.67% of HE800, HA or GY785 (i.e. 10mg/ml of basic medium) presented all the appropriate osmolarity and pH values for cell culture (Table 2). The presence of HE800 and HA in the Si-HPMC network speeded up the gelation process and this was more pronounced with HA. In the presence of GY785, gelation time was 2 times longer. Significant variations of compressive modulus were observed between each hydrogel except between those containing HE800 and HA (Fig. 1A). The addition of 0.67% of HE800 or HA increased the compressive modulus of the Si-HPMC hydrogel roughly 3 to 4 times, and the addition of 0.67% of GY785 about twice. By varying the concentration of HE800 from 0 to 0.67% (Fig. 1B), the compressive modulus significantly increased about 1.5 times with 0.17% of HE800 and about 3.5 times for concentrations greater than or equal to 0.34% of HE800. The maximal values reached a plateau of 10-12kPa. As seen on the SEM images (Fig. 2), the flash frozen-dried hydrogels all presented a porous inner structure with interconnected channels but with different spatial organization. At low and high magnifications (100 X and 2.5K X), Si-HPMC hydrogels without or with 0.67% of GY785 showed similar outer surfaces and an irregular sheet organization. At low magnification (100 X), the outer surfaces of Si-HPMC hydrogels containing 0.67% of HE800 or HA looked alike and far more dense than the other two, while their inner structures were very different, as seen at high magnification. Mixing HA with Si-HPMC effectively led to a uniform network, while Si-HPMC/HE800 (2/0.67) hydrogel showed two types of structure with many pendant bubble images.

3.3. Cell culture

Adding marine polysaccharides HE800 and GY785 at a concentration of 0.67% to the Si-HPMC hydrogel led to two new hydrogels with higher compressive moduli than Si-HPMC alone. The aim of the cellular experiments was to evaluate the ability of the hydrogels supplemented with 0.67% of HE800 or GY785 EPS to allow viability, cell attachment as well as cell repartition or cluster formation of osteoblast and chondrocyte cells culturing respectively in 2 dimensions on the top of the hydrogels or in 3 dimensions directly within it.

3.3.1. Cell viability in 2D and 3D culture

In the 2D experiments, the MTS assays (supplementary data) and the cell counting (Fig. 3A and 3B) provided comparable data and showed that no hydrogel composition tested was cytotoxic. In the 3D experiments, the hydrogels containing the HE800 EPS dramatically affected the viability of MC3T3-E1 and C28/I2 cells, particularly at a concentration of 0.67% (Fig. 4A and 4B). This high mortality was also observed with lower concentrations of HE800 (from 0.17% to 0.5%) in the case of MC3T3-E1 cultures only (Fig 4C). The results differed slightly between the two panels (Fig. 4A and 4C) which were inherent to biological variability between two different experiments. However, the cell responses within the Si-HPMC (2) and Si-HPMC/HE800 (2/0.67) hydrogels between the two panels followed the same trend and are clearly interpretable.

3.3.2. Morphology and spatial organization of cells in 2D culture

The presence of HE800, HA or GY785 within the Si-HPMC hydrogel induced the attachment of MC3T3-E1 cells even at low concentrations (Fig. 5). The dispersion of cells on to the surfaces of these types of hydrogel was even better with increased concentrations of GAG-like polysaccharides. Similar results were obtained with C28/I2 cells (results not shown). No cell attached on to the Si-HPMC hydrogel as confirmed by the counting of cells in the medium (Fig. 6). The presence of 0.67% of HE800, HA or GY785 within the Si-HPMC hydrogel allowed most of the cells to attach to the hydrogels like in 2D cultures on to tissue culture plastic (TCPS). Looking at the histochemical staining assays (Fig. 7), MC3T3-E1 cells spread better on to hydrogels containing HE800, forming clusters of 2 cells on average, than on to hydrogels containing HA or GY785, on to which they stayed round and formed clusters of 5 to 10 cells on average, respectively.

3.3.3. Morphology and spatial organization of cells in 3D culture

In 5 weeks of culture in Si-HPMC hydrogels, without or with 0.67% of HA or GY785, MC3T3-E1 cells stayed round and alive, forming clusters of only 2 or 3 cells (results not shown). In contrast to MC3T3-E1 cells, C28/I2 cells formed growing clusters of different morphology (Fig. 8). Within the Si-HPMC hydrogel, they proliferated concentrically leading to well-defined spherical clusters of about 50-55 μ m in size. Within the hydrogels containing HA or GY785, C28/I2 cells spread out more in the microenvironment, leading to clusters of about 60-100 μ m in size. The percentage of dead cells per cluster was not quantified but seemed to be low, especially in the hydrogels containing HA and GY785, as shown after calcein AM (living cells) and ethidium homodimer-1 (dead cells) assays. No yellow staining or alcian blue staining were observed, except in the presence of GY785 even without cells. C28/I2 cells cultured over 5 weeks in hydrogels containing HE800 stayed alive for concentrations ranging from 0.17% to 0.5% but cell proliferation was only observed in hydrogels containing less than 0.5% of HE800 (Fig. 9).

4. Discussion

The first step of our work was to define the best way of associating HE800, HA and GY785 polysaccharides with the Si-HPMC hydrogel without dramatically affecting its gelation process, pH and osmolarity. The preparation protocol for the Si-HPMC hydrogel was optimized to match tissue engineering applications. The two options were therefore to add the polysaccharides to the basic solution containing 3wt% of Si-HPMC (pH=12.6) or to the acid buffer (pH=3.6). Adding it to the basic solution was preferred as HE800, HA and GY785 were soluble in it but not in the acid buffer. However, saturation of the basic medium was reached with 10mg of HE800 per ml. This concentration was thus defined as the maximal working concentration and was also the one used for most of our experiments

as it led to the greatest mechanical properties (Fig. 1) while maintaining cell viability (Figs. 4A and 4B), except for the experiments with HE800 for which the concentration had to be tuned (Figs. 1B and Fig. 1C-D).

Although adding HE800, HA or GY785 did not affect the pH or osmolarity of the Si-HPMC hydrogel (Table 2), it did significantly modify its gelation time (Table 2) but with no dramatic consequences as the resulting hydrogels were all injectable and adapted for the incorporation of cells. The fact that HA speeded up the gel point by at least 17 times (Table 2) could be due to a high affinity of HA for the Si-HPMC polymer. It has effectively already been described that hyaluronic acid and cellulose derivatives can form cross-linked gel-like structures (31).

Adding 0.67% of HE800 or HA or GY785 to the Si-HPMC hydrogel significantly increased its compressive modulus, and the two structural analogs, HE800 and HA, offered similar mechanical properties (Fig. 1A). The values obtained by decreasing the concentration of HE800 from 0.67% down to 0.34% were not significantly different (Fig. 1B). In conclusion, the hydrogels containing 0.34% to 0.67% of HE800 or 0.67% of HA offered the highest compressive moduli at $10.25 \text{ kPa} \pm 0.75$. These constructions were the most interesting in terms of mechanical properties as the value of their compressive modulus is similar to that of native cartilage, estimated at about 20kPa (32).

Authors who want to show the effect of peptide grafting on hydrogel macromolecules on cell attachment use 2 dimensional cell cultures on the surface of the modified hydrogels (33, 34). They compare 2 dimensional cell culture on the surface of the hydrogels with 3 dimensional cell culture encapsulated inside the synthetic structure. The 2 dimensional experiments make it possible to visualize the cells spreading on a surface. Inside the hydrogel, the structure is isotropic without any preferential direction (35). If the cell membrane links the RGD structures of the hydrogel by means of its integrin receptors, it is not visible because the cell attached within the hydrogel stays round without any 2 dimensional surfaces to follow. A paper by Lei *et al.* (36) reports that RGD concentration influenced the extent of cell spreading. A large percentage of cells remained spherical after 3 days of culture inside the hydrogels with low RGD concentrations (RGD 100, 250 μM). If the RGD concentrations become very high, most of the cells can spread inside the hydrogels with high RGD concentrations (RGD 750, 1000 μM), although it was difficult to quantify the extent of the spreading. However, it was generally observed that the cells were much longer and extended into the hydrogels with more RGD. In a macroporous hydrogel made, using a simultaneous gas-foaming, free-radical crosslinking approach (37), the cells are inside macropores on the surface of the hydrogel as in the 2 dimensional experiments but in a specific microenvironment and can spread on the surface of the hydrogel. On the contrary, if fibrillar proteins, such as collagen, or solid granules, such as calcium phosphate (38), are added to a hydrogel, with cells, the material is anisotropic or biphasic and the cells spread on the surface of the fibril or the granules. In our case, the macromolecules added into the Si-HPMC hydrogel were soluble in it and the structure was isotropic without any direction or surface for the cells to attach to. If we wanted to follow cell attachment, adhesion and spreading on modified uniform hydrogels, we would have needed to observe cells on the surface. The presence of HA, HE800 and GY785 in the Si-HPMC hydrogel induced the attachment of MC3T3-E1 and C28/I2 cells when these cells were cultured in 2D on top of the hydrogels (Fig. 5). Elsewhere (39) it has been described that cell attachment and cell spreading are linked to the stiffness and electric charge of the surface. Indeed, in our experiments, the best cell dispersion and cell spreading (Figs. 5 and 7) were observed on the hydrogels with the highest compressive modulus (Fig. 1) and densest surface structure (Fig. 2) (i.e. Si-HPMC hydrogels supplemented with 0.67% of HE800 or HA). Also, cell attachment was only observed on the hydrogels containing HE800, HA and GY785, which are negatively charged polymers, contrary to Si-HPMC which is neutral. As described in the literature (24, 40, 41), negatively charged polymers promote the adsorption of proteins by interacting ionically with their cationic amino acids. Also, many papers relate that HA polysaccharide promotes cell adhesion and mobility by interacting specifically with the RHAMM cell receptor and the CD44 cell receptor, which binds to a six to ten-sugar sequence of HA (24, 42). It would therefore be interesting to investigate whether HE800 and GY785 EPSs have such specific interactions by using surface plasmon resonance technology for example.

In the 3D experiments (Fig 4), cell death was only observed in Si-HPMC hydrogels containing HE800, while no adverse effect was noticed in 2D cytotoxicity assays with this polysaccharide (Fig. 5). This cellular death was therefore not related to the HE800 polysaccharide itself. Nor was it due to a high compressive modulus as the cells cultured in hydrogels with equal compressive modulus, such as Si-HPMC hydrogels containing 0.67% of HE800 or 0.67% of HA (Fig 1A), showed either a low mortality with HA or a high mortality with HE800 (Figs. 4A and 4B). This cell death could be related to the inner structure of the hydrogel and particularly to the spatial organization of HE800. As has been well documented in the literature, mean pore size in the scaffolds is the key point for obtaining a

biologically active material (43). The pore should be greater than 20 μ m and less than 120 μ m if it is to provide cell attachment and viability in the scaffolds; a linear relationship has been found between cell attachment and specific surface area, and there is an optimal pore size or range for each distinct cell type (44). As noted by Vickers *et al.*, the decrease in pore diameter attendant to scaffold contraction has been documented histologically. The concept of dynamic pore reduction was presented previously as an approach for achieving a desired cell density by means of pore volume reduction resulting from cell-mediated contraction of porous scaffolds of lower stiffness (45). In our study, the Si-HPMC hydrogel was not a highly porous or macroporous scaffold. Cells are not seeded inside hydrogel macropores but encapsulated inside the network. We only have nanopores to enable the diffusion of gas and nutrients. Pores are visible under scanning microscopy because water is removed in the course of the technical preparation. These SEM pictures reveal artifacts and not the real structures but these artifacts are linked to the real structures and the density of the hydrated gels. These pores revealed the viscoelasticity and ability of the macromolecule network to be strained when the water is removed before being analyzed in the SEM. As shown in the SEM images (fig.2), pore size seemed to increase when hyaluronic acid or GY785 EPS was added to the Si-HPMC hydrogel (the pore size was about 25 μ m) and the pores seemed to be interconnected. The size of these pores was far higher than that of individual cells (5-7 μ m), therefore cell infiltration and migration should be possible if cells can strain the structure. On the other hand, when HE800 was added to the Si-HPMC hydrogel, the hydrogel seemed less porous and no pores were observed inside the hydrogel as observed in the respective SEM images at high magnification (Fig. 2), suggesting a three-dimensional (3D) structure that is unsuitable for promoting cell proliferation and viability. The hydrogel containing 0.67% of HE800 had a dense inner structure (Fig. 2) that may lead to poor permeability (46) and consequently to slow diffusion of nutrients and gases. The concentration of HE800 was consequently lowered to check whether this would benefit cell viability (Figs. 4C and 4D) while maintaining high mechanical properties (Fig. 1B). Results showed that this was true only with C28/I2 cells and particularly with the Si-HPMC hydrogel containing 0.34% of HE800.

In 3D culture, only the C28/I2 cells proliferated. MC3T3-E1 is a mouse osteoblastic cell line and, as with many cell types, they need to interact and adhere and bind ligands in their micro-environment to proliferate (38, 47, 48). In this study, the marine polysaccharides added to the Si-HPMC hydrogel did not seem to produce an adhesion site, even after 3 weeks of culture, and the MC3T3-E1 cells remained round. Depending on the construction, the morphology of the C28/I2 cells was different. Cell growth varied with the nature of both the hydrogel and polysaccharide (Figs. 8 and 9). In the Si-HPMC hydrogel, the cells clustered together whereas in the presence of hyaluronic acid or GY785 EPS, the cells spread out more in the microenvironment. The hydrogels containing 0.67% of HE800 or GY785 marine polysaccharides had a compressive modulus 3 and 2 times higher than Si-HPMC hydrogel alone, respectively. Therefore, they both have interesting mechanical properties, as expected. Their benefit, however, in terms of biological responses, is different. Indeed, as seen by the 2D culture experiments, both HE800 and GY785 made it possible to retain most of the cells on the surface of the hydrogels after culture medium removal, but the benefit of HE800 was that it induced cell spreading. In 3D experiments, the GY785 had the most benefit, which was to make cell viability and proliferation possible. In conclusion, HE800 seemed more adapted to 2D cell cultures (for patches for example) and GY785 for use as a 3D scaffold for cell cultures.

5. Conclusion

The two GAG-like marine exopolysaccharides, HE800 and GY785 were associated with an Si-HPMC hydrogel to assess both the mechanical and biological properties of the new hydrogels built. HE800 and GY785 polysaccharides significantly improved the mechanical properties of the Si-HPMC hydrogel and induced the attachment of MC3T3-E1 and C28/I2 cells when these were cultured in 2D on top of the hydrogels. HE800 had the highest compressive modulus (11kPa) and allowed the best cell dispersion, especially with MC3T3-E1 when cultured on top of the hydrogels. Of all the constructs tested, the Si-HPMC hydrogels containing 0.34% of HE800 or 0.67% of GY785 or 0.67% of HA presented the most interesting features for cartilage tissue engineering applications as they offered the highest compressive modulus (9.5-11kPa) while supporting the proliferation of chondrocytes. The hydrogel supplemented with 0.67% of HE800 had the best cell spreading in two dimensions and will be used in the form of a patch.

Acknowledgements

We acknowledge IFREMER and the *Pays de la Loire* council for their financial support through the Bioregos grant and PhD studentship (Emilie Rederstorff). We also thank Christophe Brandily for the chemical structure representation of the polysaccharides, Sandrine Lavenus for her help in histochemical staining, Caroline Colombeix for her help in using the confocal microscope and Gilles Fanchon for the osmolarity measurements.

References

1. Puppi D, Chiellini F, Piras AM, Chiellini E. Polymeric materials for bone and cartilage repair. *Progress in Polymer Science*;35(4):403-40.
2. Dang JM, Leong KW. Natural polymers for gene delivery and tissue engineering. *Advanced Drug Delivery Reviews*2006;58(4):487-99.
3. Nair LS, Laurencin CT. Biodegradable polymers as biomaterials. *Progress in Polymer Science* 2007/9//;32(8-9):762-98.
4. Muzzarelli RAA. Chitins and chitosans for the repair of wounded skin, nerve, cartilage and bone. *Carbohydrate Polymers*2009;76(2):167-82.
5. Di Martino A, Sittinger M, Risbud MV. Chitosan: A versatile biopolymer for orthopaedic tissue-engineering. *Biomaterials*2005;26(30):5983-90.
6. Francis Suh JK, Matthew HWT. Application of chitosan-based polysaccharide biomaterials in cartilage tissue engineering: a review. *Biomaterials*2000;21(24):2589-98.
7. Li Z, Ramay HR, Hauch KD, Xiao D, Zhang M. Chitosan-alginate hybrid scaffolds for bone tissue engineering. *Biomaterials*2005;26(18):3919-28.
8. Stevens MM, Qanadilo HF, Langer R, Prasad Shastri V. A rapid-curing alginate gel system: utility in periosteum-derived cartilage tissue engineering. *Biomaterials*2004;25(5):887-94.
9. Müller FA, Müller L, Hofmann I, Greil P, Wenzel MM, Staudenmaier R. Cellulose-based scaffold materials for cartilage tissue engineering. *Biomaterials*2006;27(21):3955-63.
10. Jin R, Moreira Teixeira LS, Dijkstra PJ, van Blitterswijk CA, Karperien M, Feijen J. Enzymatically-crosslinked injectable hydrogels based on biomimetic dextran-hyaluronic acid conjugates for cartilage tissue engineering. *Biomaterials*;31(11):3103-13.
11. Barbucci R, Lamponi S, Borzacchiello A, Ambrosio L, Fini M, Torricelli P, et al. Hyaluronic acid hydrogel in the treatment of osteoarthritis. *Biomaterials*2002 Dec;23(23):4503-13.
12. Kim J, Kim IS, Cho TH, Lee KB, Hwang SJ, Tae G, et al. Bone regeneration using hyaluronic acid-based hydrogel with bone morphogenic protein-2 and human mesenchymal stem cells. *Biomaterials*2007;28(10):1830-7.
13. Yoo HS, Lee EA, Yoon JJ, Park TG. Hyaluronic acid modified biodegradable scaffolds for cartilage tissue engineering. *Biomaterials*2005;26(14):1925-33.
14. Chen Y-L, Lee H-P, Chan H-Y, Sung L-Y, Chen H-C, Hu Y-C. Composite chondroitin-6-sulfate/dermatan sulfate/chitosan scaffolds for cartilage tissue engineering. *Biomaterials*2007;28(14):2294-305.
15. Rigouin C, Ladrat CD, Sinquin C, Collic-Jouault S, Dion M. Assessment of biochemical methods to detect enzymatic depolymerization of polysaccharides. *Carbohydrate Polymers*2009;76(2):279-84.
16. Raguènes G, Christen R, Guezennec J, Pignet P, Barbier G. *Vibrio diabolicus* sp. nov., a New Polysaccharide-Secreting Organism Isolated from a Deep-Sea Hydrothermal Vent Polychaete Annelid, *Alvinella pompejana*. *Int J Syst Bacteriol*1997;47(4):989-95.
17. Collic-Jouault S, Chevotot L, Helley D, Ratiskol J, Bros A, Sinquin C, et al. Characterization, chemical modifications and in vitro anticoagulant properties of an exopolysaccharide produced by *Alteromonas infernus*. *Biochimica et Biophysica Acta (BBA) - General Subjects*2001;1528(2-3):141-51.
18. Raguènes G, Peres A, Ruimy R, Pignet P, Christen R, Loaec M, et al. *Alteromonas infernus* sp. nov., a new polysaccharide-producing bacterium isolated from a deep-sea hydrothermal vent. *Journal of Applied Microbiology*1997;82(4):422-30.
19. Rougeaux H, Kervarec N, Pichon R, Guezennec J. Structure of the exopolysaccharide of *Vibrio diabolicus* isolated from a deep-sea hydrothermal vent. *Carbohydrate Research*1999;322(1-2):40-5.

20. Roger O, Kervarec N, Ratiskol J, Collicec-Jouault S, Chevolut L. Structural studies of the main exopolysaccharide produced by the deep-sea bacterium *Alteromonas infernus*. *Carbohydrate Research*2004;339(14):2371-80.
21. Gandhi NS, Mancera RL. The Structure of Glycosaminoglycans and their Interactions with Proteins. *Chemical Biology & Drug Design*2008;72(6):455-82.
22. Lord MS, Pasqui D, Barbucci R, Milthorpe BK. Protein adsorption on derivatives of hyaluronic acid and subsequent cellular response. *Journal of Biomedical Materials Research Part A*2009;91A:635-46.
23. Zanchetta P, Lagarde N, Guezennec J. Systemic Effects on Bone Healing of a New Hyaluronic Acid-Like Bacterial Exopolysaccharide. *Calcified Tissue International*2003;73(3):232-6.
24. Morra M. Engineering of Biomaterials Surfaces by Hyaluronan. *Biomacromolecules*2005;6(3):1205-23.
25. Fatimi A, Tassin JF, Quillard S, Axelos MA, Weiss P. The rheological properties of silated hydroxypropylmethylcellulose tissue engineering matrices. *Biomaterials*2008;29(5):533-43.
26. Laïb S, Fella BH, Fatimi A, Quillard S, Vinatier C, Gauthier O, et al. The in vivo degradation of a ruthenium labelled polysaccharide-based hydrogel for bone tissue engineering. *Biomaterials*2009;30(8):1568-77.
27. Vinatier C, Magne D, Weiss P, Trojani C, Rochet N, Carle GF, et al. A silanized hydroxypropyl methylcellulose hydrogel for the three-dimensional culture of chondrocytes. *Biomaterials*2005 Nov;26(33):6643-51.
28. Trojani C, Boukhechba F, Scimeca J-C, Vandenbos F, Michiels J-F, Daculsi G, et al. Ectopic bone formation using an injectable biphasic calcium phosphate/Si-HPMC hydrogel composite loaded with undifferentiated bone marrow stromal cells. *Biomaterials*2006;27(17):3256-64.
29. Bourges X, Weiss P, Daculsi G, Legeay G. Synthesis and general properties of silated-hydroxypropyl methylcellulose in prospect of biomedical use. *Advances in Colloid and Interface Science*2002;99(3):215-28.
30. Fatimi A, Tassin J-F, Turczyn R, Axelos MAV, Weiss P. Gelation studies of a cellulose-based biohydrogel: The influence of pH, temperature and sterilization. *Acta Biomaterialia*2009;5(9):3423-32.
31. Hoare TR, Kohane DS. Hydrogels in drug delivery: Progress and challenges. *Polymer*2008;49(8):1993-2007.
32. Discher DE, Mooney DJ, Zandstra PW. Growth Factors, Matrices, and Forces Combine and Control Stem Cells. *Science*2009 June 26, 2009;324(5935):1673-7.
33. Shu XZ, Ghosh K, Liu Y, Palumbo FS, Luo Y, Clark RA, et al. Attachment and spreading of fibroblasts on an RGD peptide-modified injectable hyaluronan hydrogel. *J Biomed Mater Res A*2004 Feb 1;68(2):365-75.
34. Schneider GB, English A, Abraham M, Zaharias R, Stanford C, Keller J. The effect of hydrogel charge density on cell attachment. *Biomaterials*2004 Jul;25(15):3023-8.
35. Nuttelman CR, Tripodi MC, Anseth KS. Synthetic hydrogel niches that promote hMSC viability. *Matrix Biol*2005 May;24(3):208-18.
36. Lei Y, Gojgini S, Lam J, Segura T. The spreading, migration and proliferation of mouse mesenchymal stem cells cultured inside hyaluronic acid hydrogels. *Biomaterials* Jan;32(1):39-47.
37. Behraves E, Mikos AG. Three-dimensional culture of differentiating marrow stromal osteoblasts in biomimetic poly(propylene fumarate-co-ethylene glycol)-based macroporous hydrogels. *J Biomed Mater Res A*2003 Sep 1;66(3):698-706.
38. Sohier J, Corre P, Weiss P, Layrolle P. Hydrogel/calcium phosphate composites require specific properties for three-dimensional culture of human bone mesenchymal cells. *Acta Biomater*2010 Aug;6(8):2932-9.
39. Boyan BD, Hummert TW, Dean DD, Schwartz Z. Role of material surfaces in regulating bone and cartilage cell response. *Biomaterials*1996;17(2):137-46.
40. Goetinck P, Stirpe N, Tsonis P, Carlone D. The tandemly repeated sequences of cartilage link protein contain the sites for interaction with hyaluronic acid. *J Cell Biol*1987 November 1, 1987;105(5):2403-8.
41. Hascall VC, Heinegard D. Aggregation of Cartilage Proteoglycans. *Journal of Biological Chemistry*1974;249(13):4232-41.
42. Underhill C. CD44: the hyaluronan receptor. *J Cell Sci*1992 October 1, 1992;103(2):293-8.
43. Yang B, Yin Z, Cao J, Shi Z, Zhang Z, Song H, et al. In vitro cartilage tissue engineering using cancellous bone matrix gelatin as a biodegradable scaffold. *Biomed Mater*2010 Aug;5(4):045003.
44. O'Brien FJ, Harley BA, Yannas IV, Gibson LJ. The effect of pore size on cell adhesion in collagen-GAG scaffolds. *Biomaterials*2005 Feb;26(4):433-41.

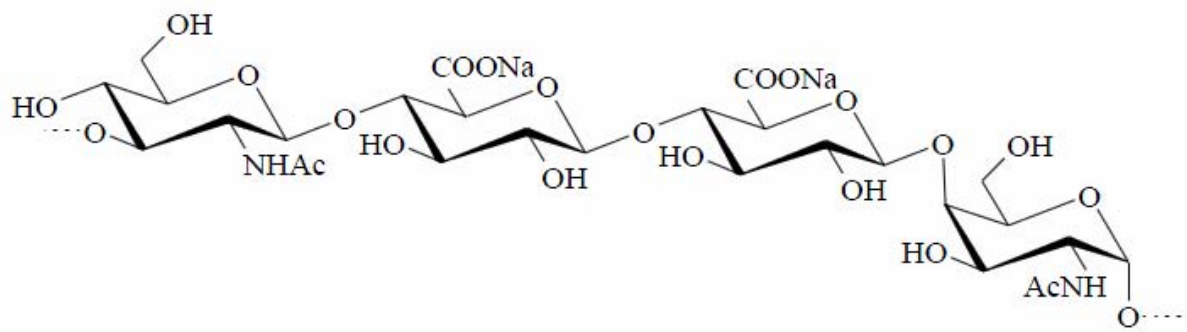
45. Vickers SM, Gotterbarm T, Spector M. Cross-linking affects cellular condensation and chondrogenesis in type II collagen-GAG scaffolds seeded with bone marrow-derived mesenchymal stem cells. *J Orthop Res*2010 Sep;28(9):1184-92.
46. Scherer GW. Influence of Viscoelasticity and Permeability on the Stress Response of Silica Gel. *Langmuir*1996;12(5):1109-16.
47. Lutolf MP, Hubbell JA. Synthetic biomaterials as instructive extracellular microenvironments for morphogenesis in tissue engineering. *Nat Biotechnol*2005 Jan;23(1):47-55.
48. Cushing MC, Anseth KS. Materials science. Hydrogel cell cultures. *Science*2007 May 25;316(5828):1133-4.

Table 1: Physico-chemical characteristics of HE800, hyaluronic acid (HA) and GY785 polysaccharides.

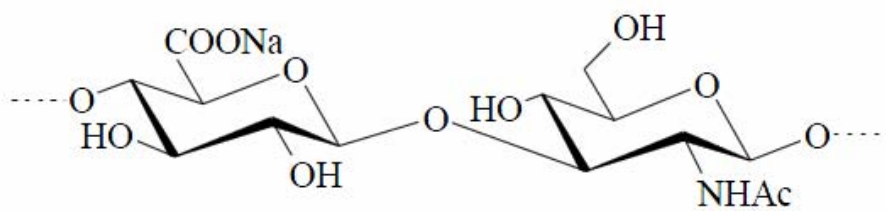
	HE800	HA	GY785
Sulfur (g/100g)	0	0	3.2
Sugar acids (g/100g)	32	30	22
I (Mw/Mn)	1.098	1.054	1.18
Mw (g/mol)	$7,4 \cdot 10^5$	$7,4 \cdot 10^5$	$1,4 \cdot 10^6$
Radius of gyration (nm)	70	108	117

Table 2: Osmolarity, pH and gel point of Si-HPMC hydrogels without or with 0.67% of HE800 or HA or GY785.

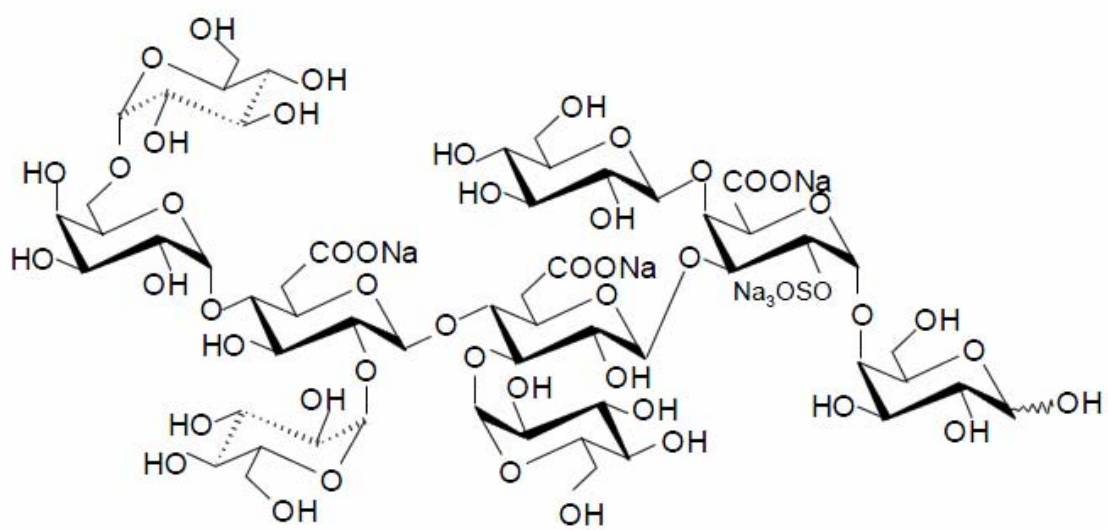
	Osmolarity (mOsm/L)	pH	Gel point (s)
Si-HPMC (2)	467	7.41	1000
Si-HPMC/HE800 (2/0.67)	455	7.39	821
Si-HPMC/HA (2/0.67)	465	7.39	<60
Si-HPMC/GY785 (2/0.67)	453	7.46	2002



HE800



Hyaluronic acid (HA)



GY785

Figure 1: Chemical structure of HE800, hyaluronic acid (HA) and GY785 polysaccharides.

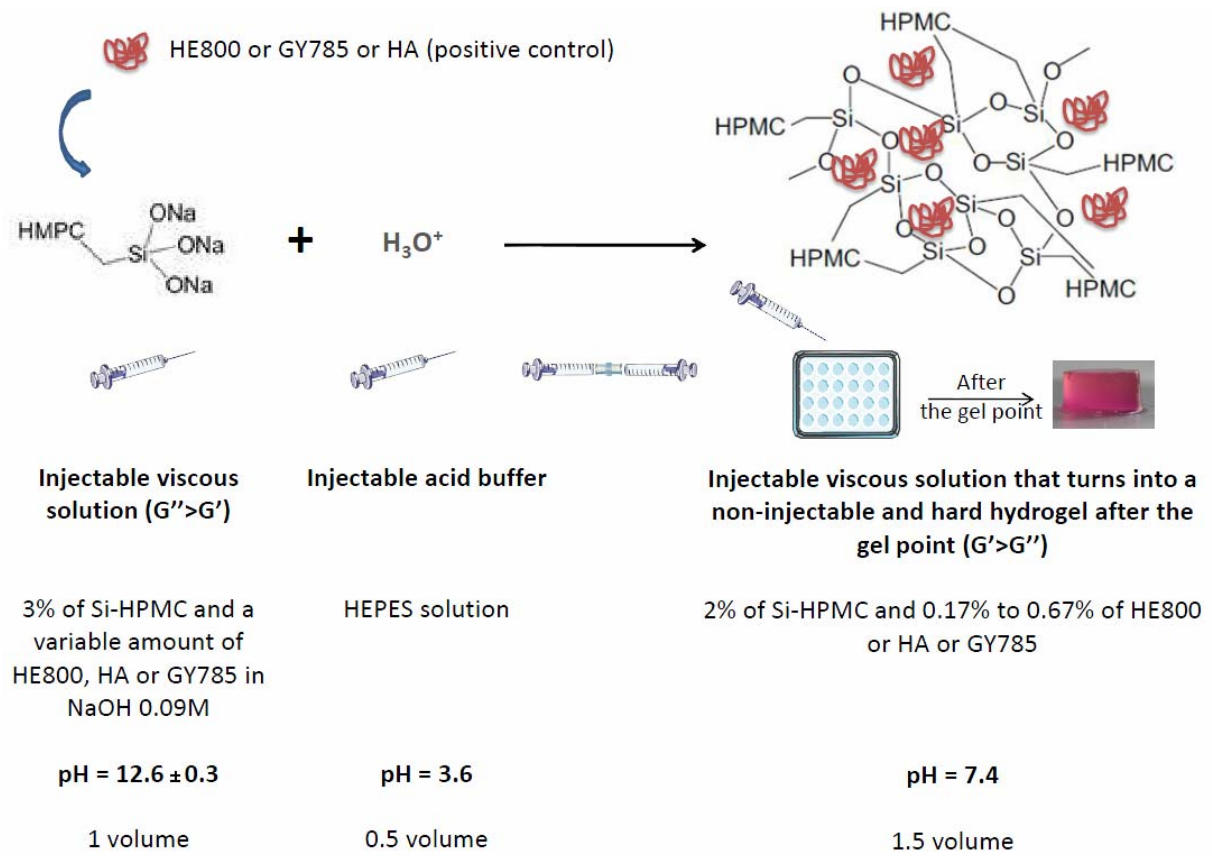


Figure 2: Scheme of the preparation of the hydrogels.

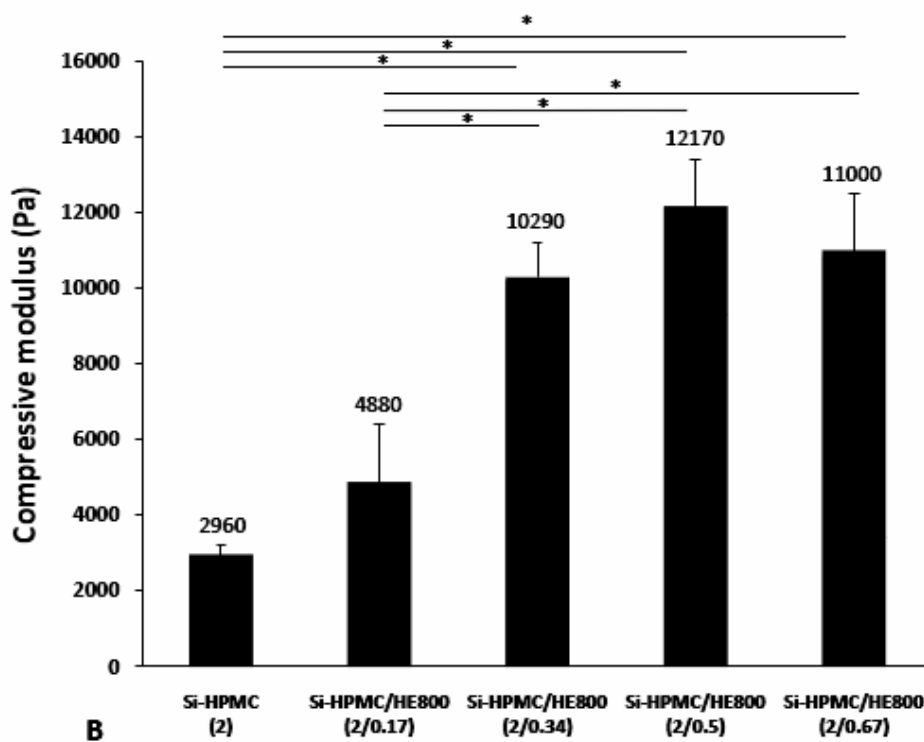
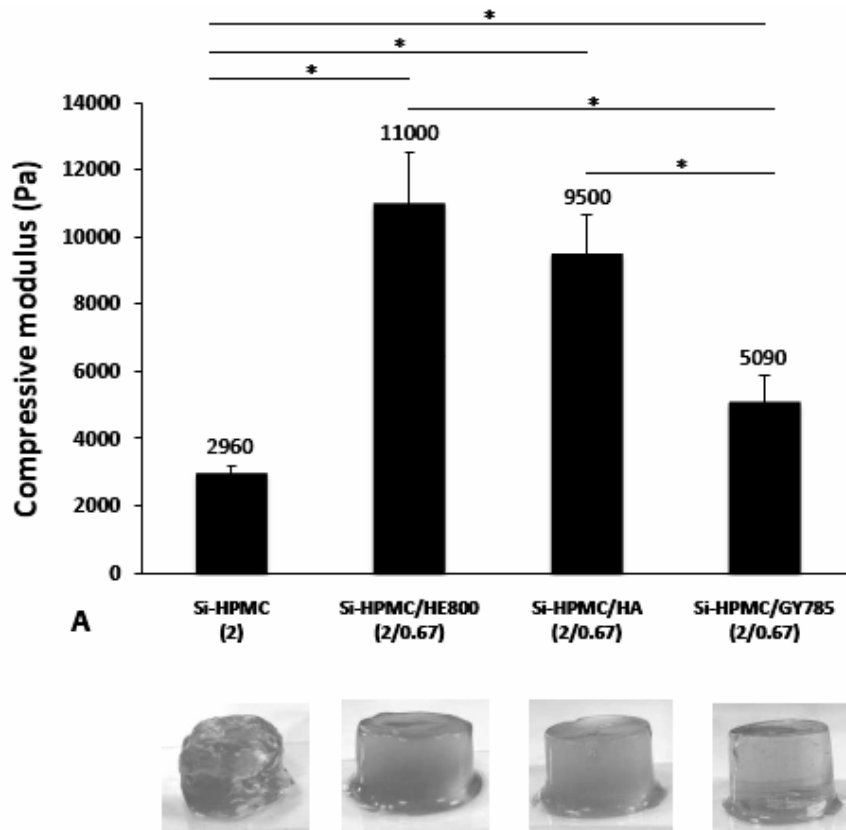


Figure 3: (A) Compressive moduli of Si-HPMC hydrogels without or with 0.67% of HE800 or HA or GY785; (B) Compressive moduli of Si-HPMC hydrogels without or with HE800 at various concentrations. * $P < 0.001$

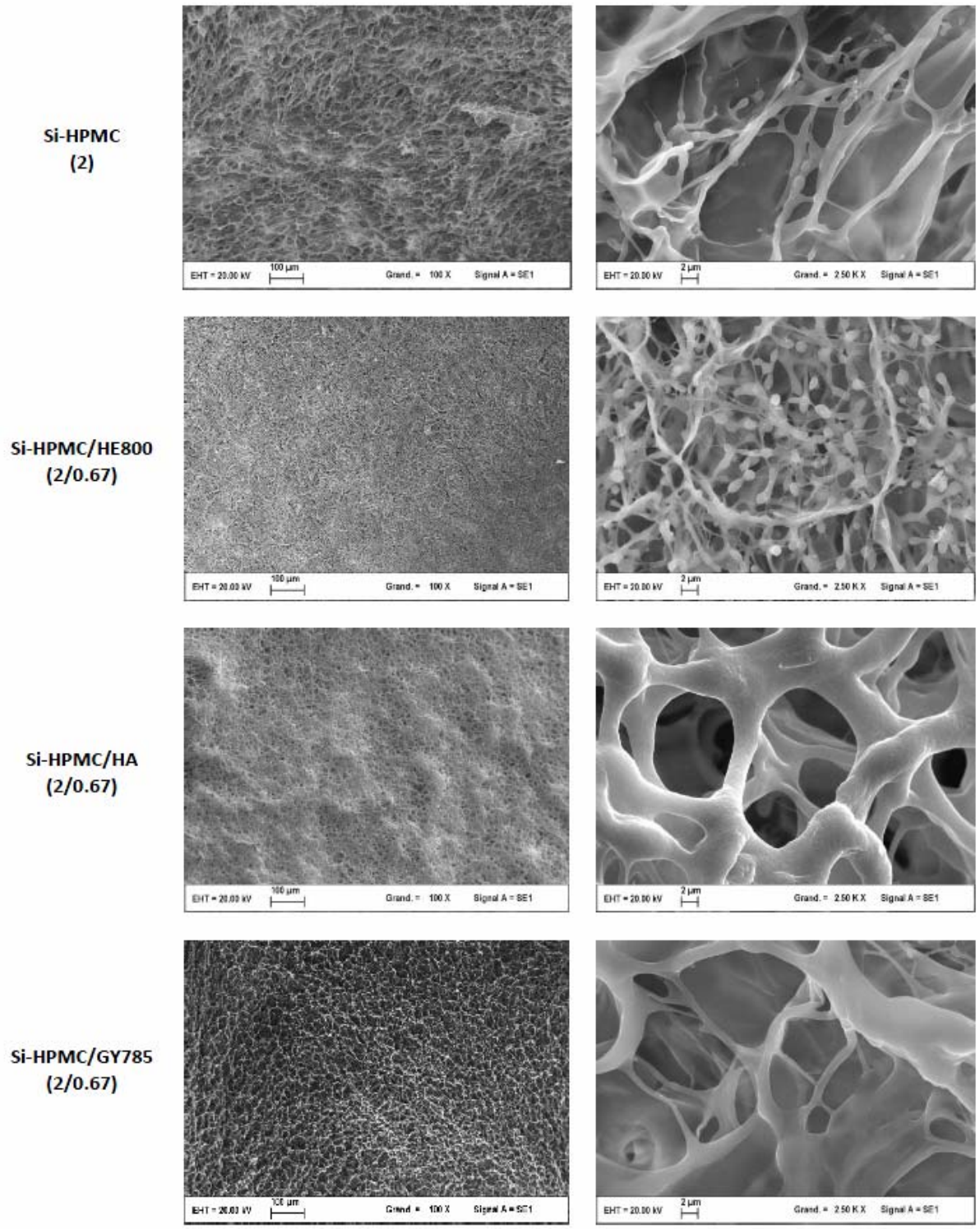


Figure 4: SEM images of flash-frozen dried hydrogels at low (100 X) and high (2.5K X) magnifications.

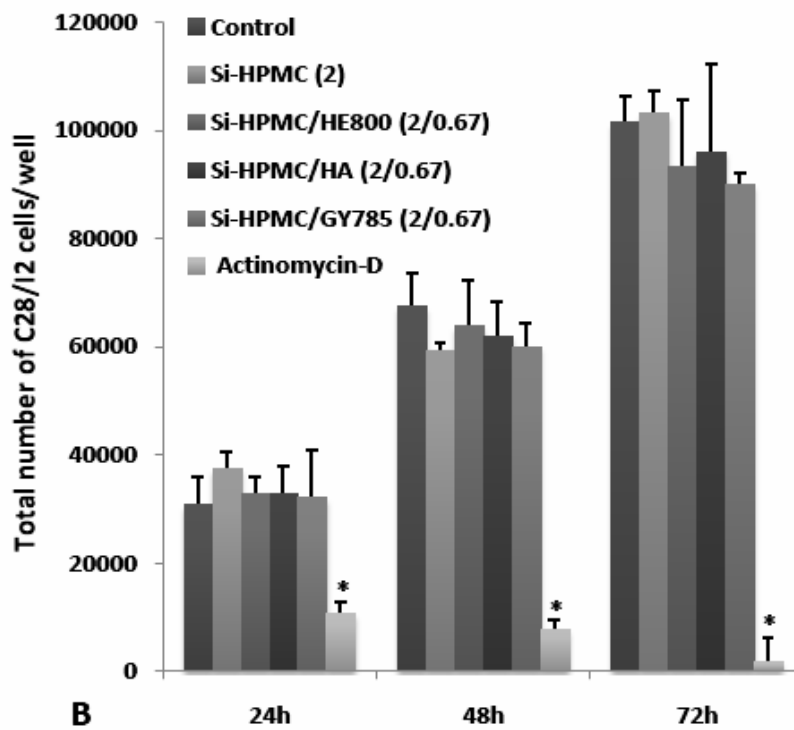
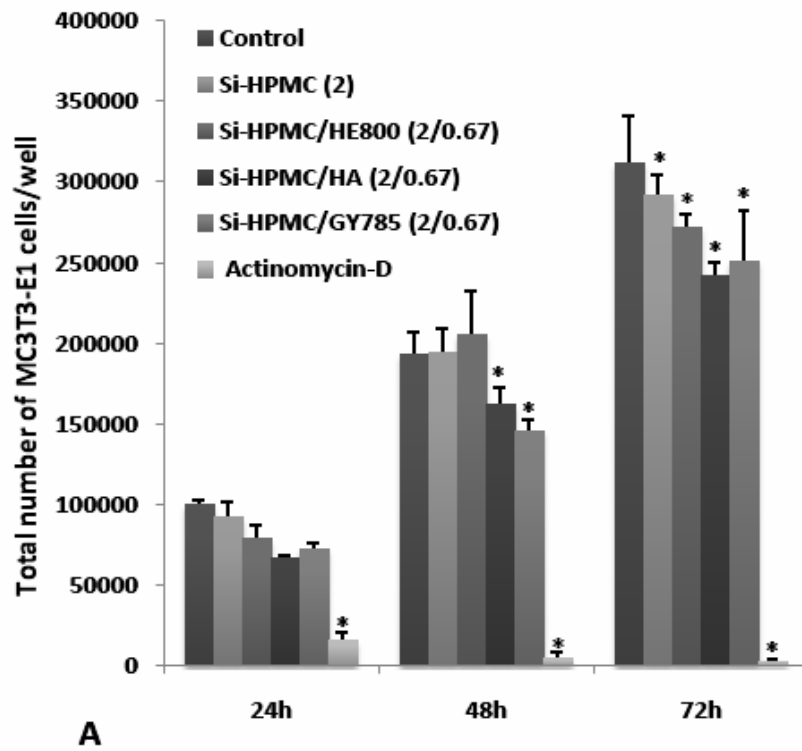


Figure 5: Proliferation of (A) MC3T3-E1 and (B) C28/12 cells cultured in 2D on culture plate over 72h in the absence of hydrogel (positive control) or in the presence of Si-HPMC (2), Si-HPMC/HE800 (2/0.67), Si-HPMC/HA (2/0.67), Si-HPMC/GY785 (2/0.67) hydrogels or in the presence of 5 μ g/ml of actinomycin-D (negative control). Results are expressed as the total number of cells per well. * $P < 0.001$ (* alone = significantly different from each other sample)

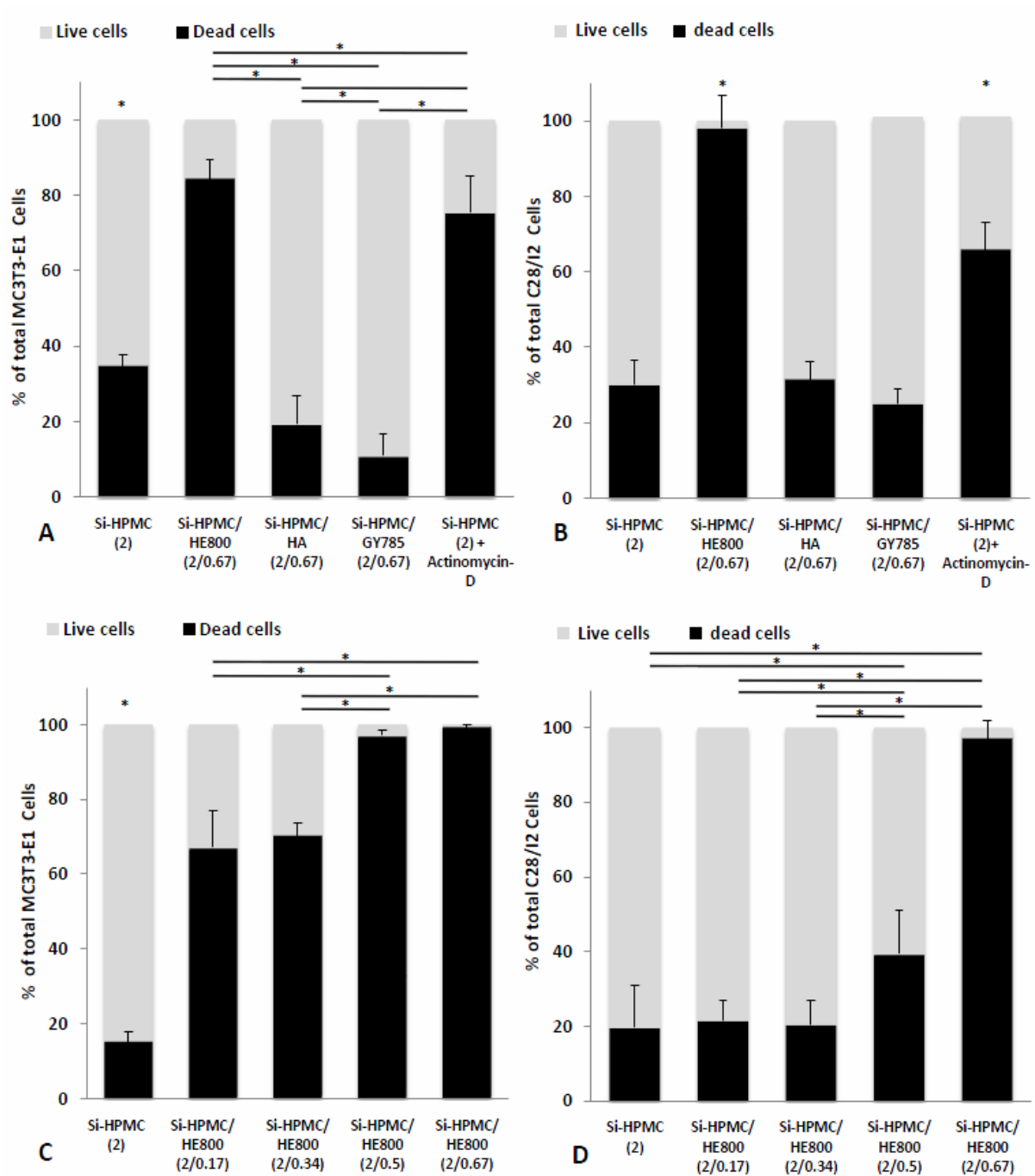


Figure 6: Percentages of living and dead cells cultured in 3D within different hydrogels over 48h: (A) MC3T3-E1 and (B) C28/I2 within Si-HPMC hydrogels without or with 0.67% of HE800 or HA or GY785, or within Si-HPMC hydrogel in the presence of actinomycin-D in the culture medium (5µg/ml); (C) MC3T3-E1 and (D) C28/I2 within Si-HPMC hydrogels without or with HE800 at various concentrations. * $P < 0.001$ (* alone = significantly different from each other sample)

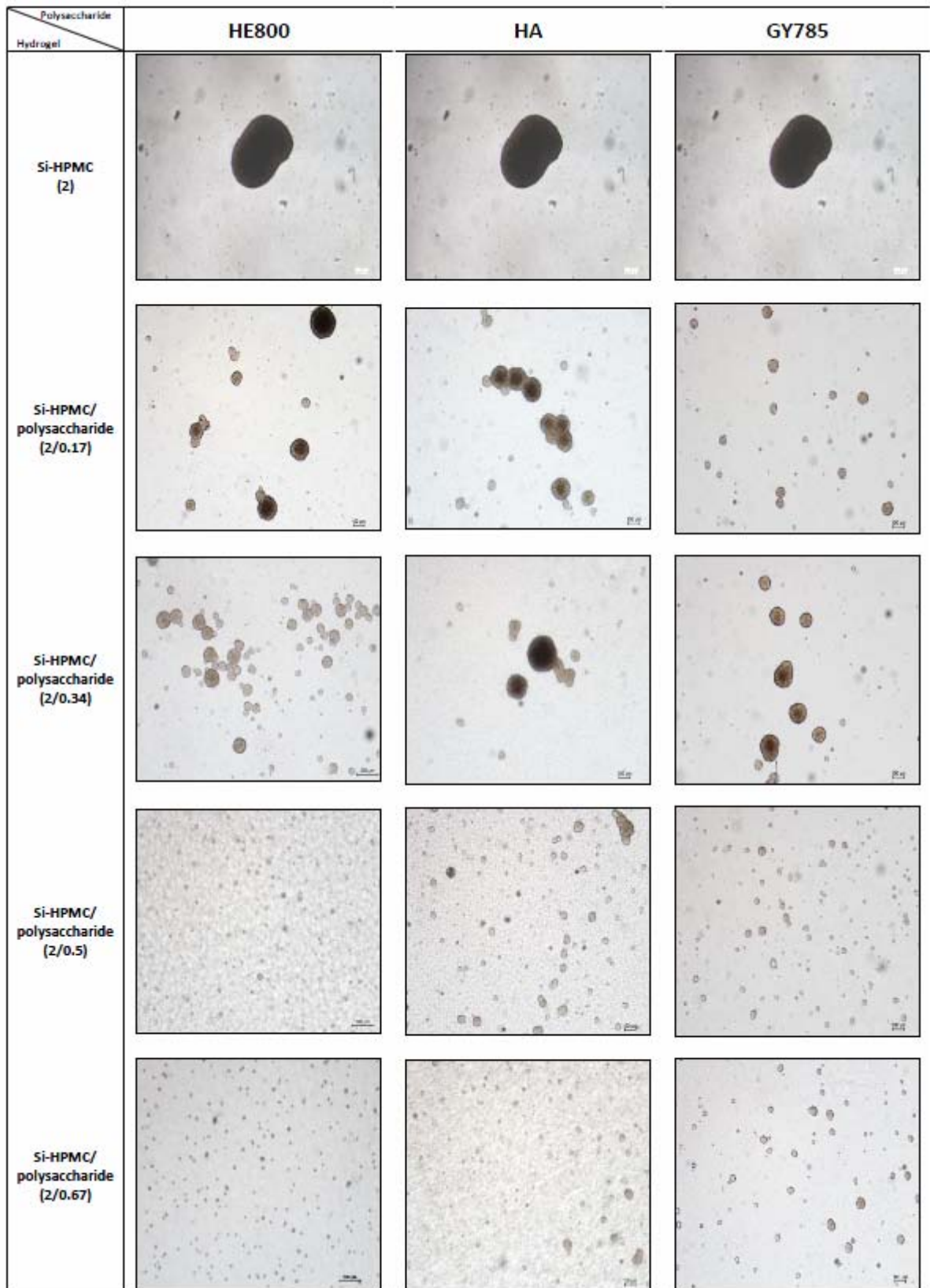


Figure 7: Optical microscope images of MC3T3-E1 cells cultured over 48h in 2D on the top of Si-HPMC hydrogels without or with HE800 or GY785 at various concentrations. (*Magnification 100 X*)

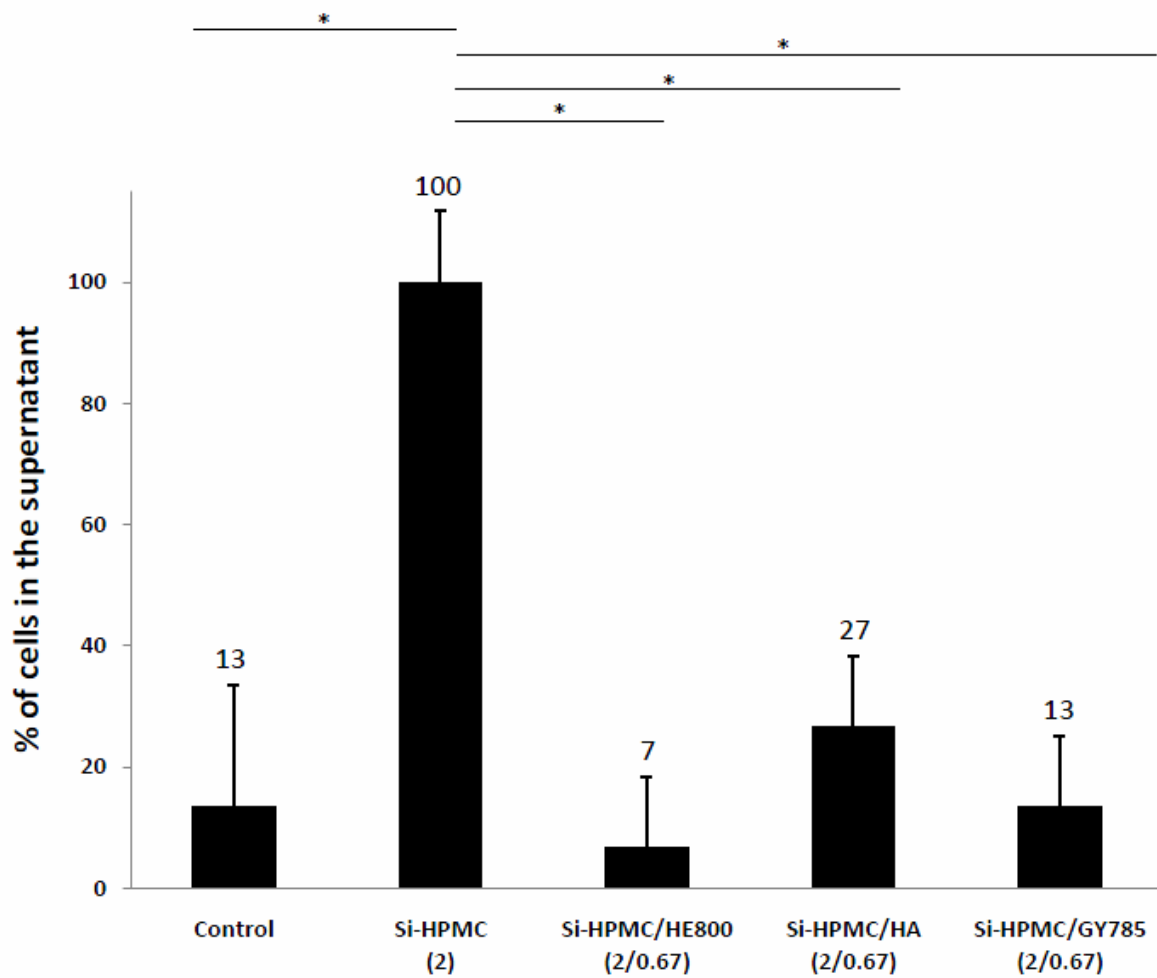


Figure 8: Percentage of MC3T3-E1 cells that remained in the culture medium 48h after culturing them in 2D onto culture plate (positive control) or on the top of Si-HPMC hydrogels without or with 0.67% of HE800 or HA or GY785. **P<0.001*

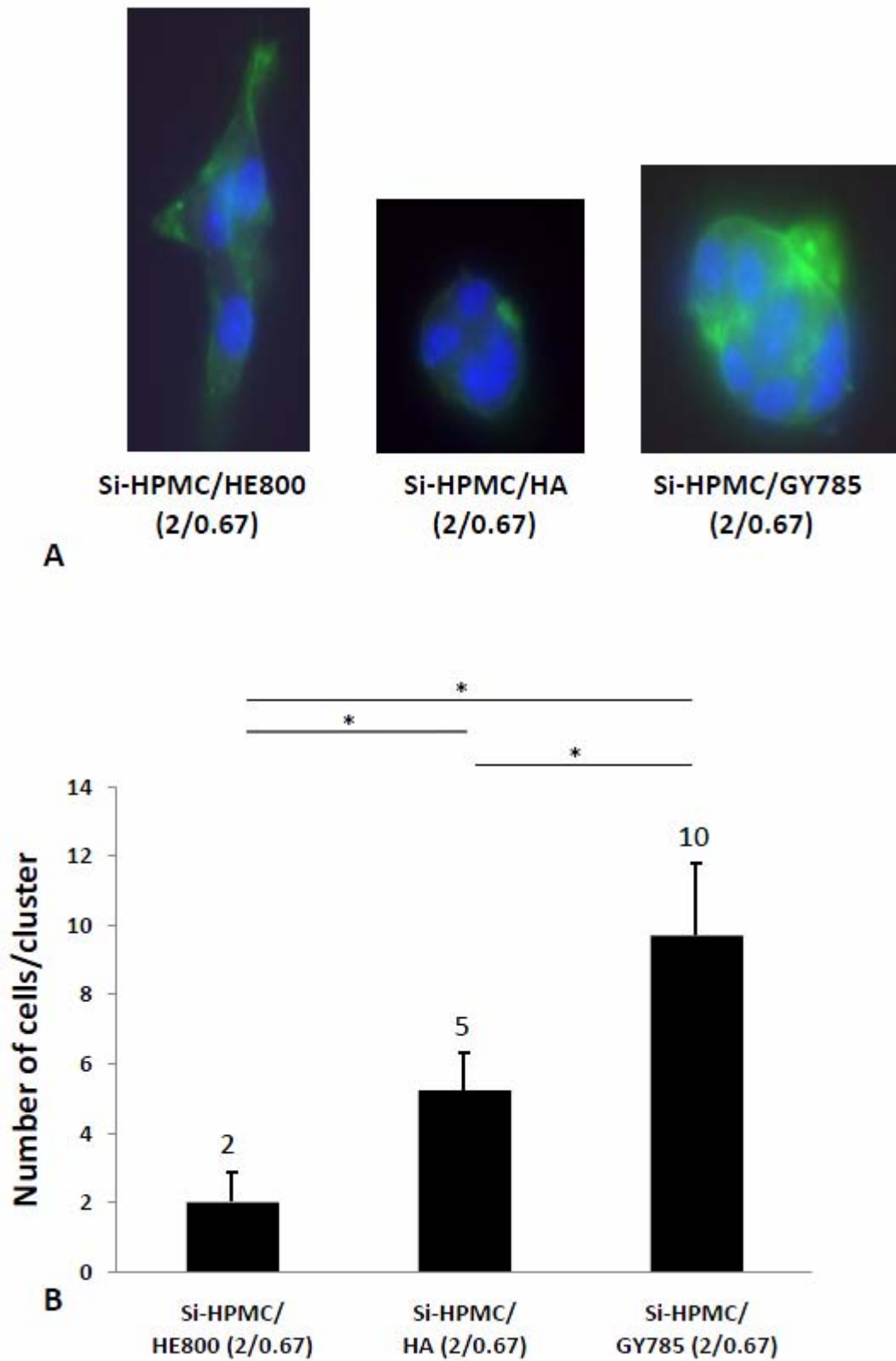


Figure 9: (A) Fluorescent images of stained MC3T3-E1 cells cultured over 48h in 2D on the top of Si-HPMC hydrogels containing 0.67% of HE800 or HA or GY785. Nuclei are in blue and actin fibers in green (B) Number of MC3T3-E1 cells per cluster. $*P < 0.001$

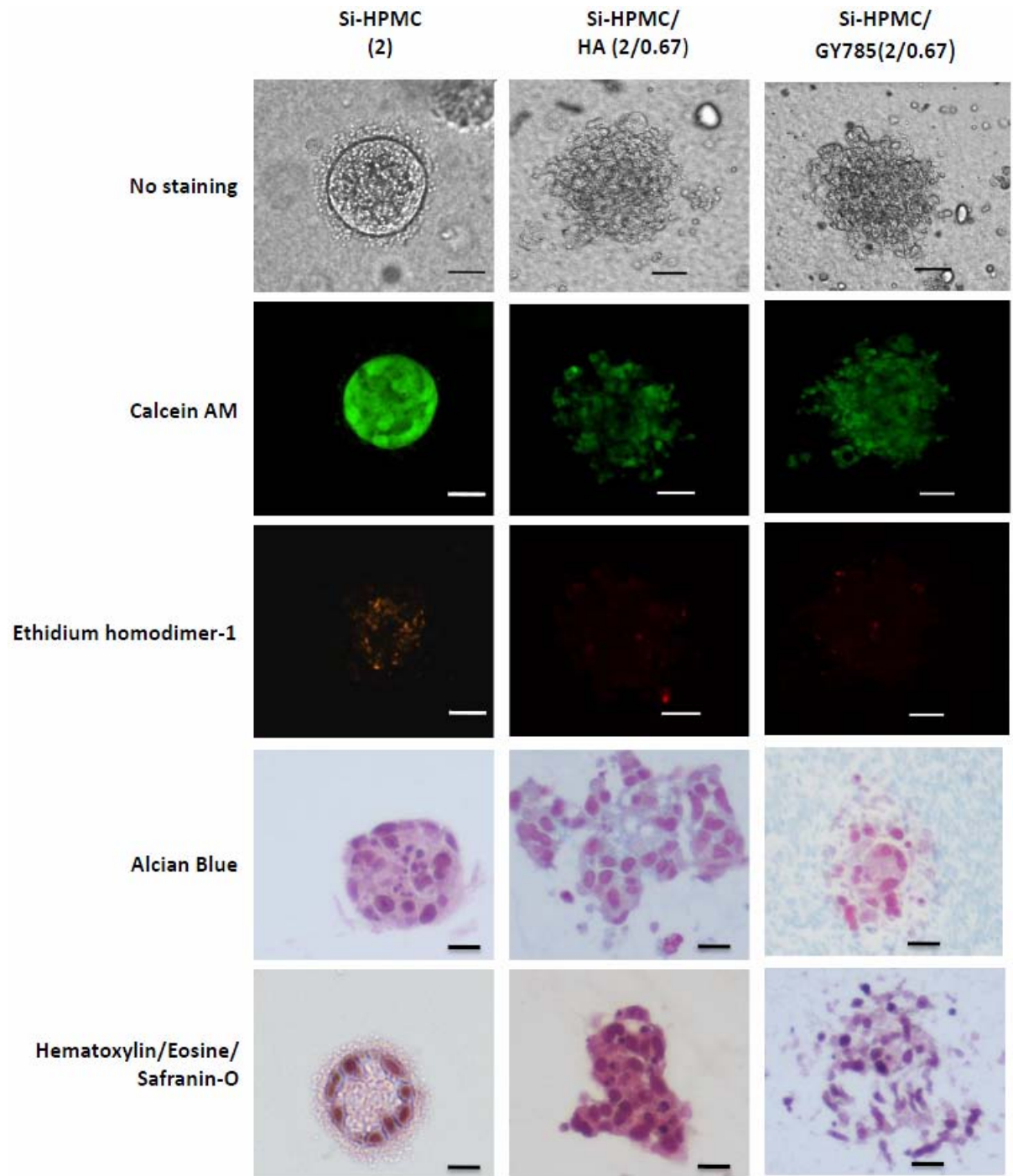
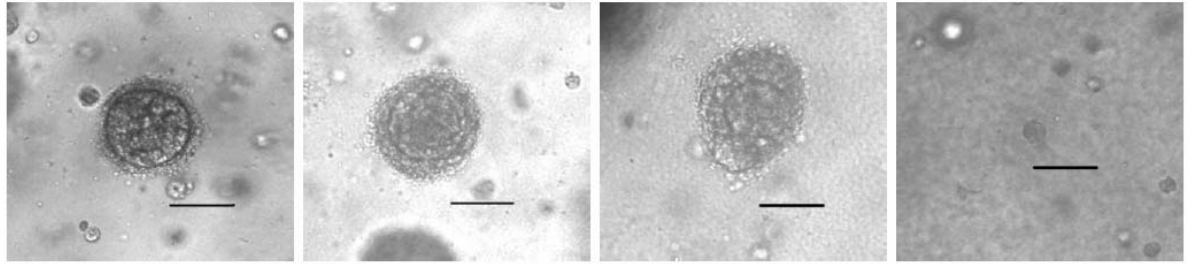


Figure 10: Optical and fluorescent images of C28/12 cells cultured over 5 weeks in 3D within Si-HPMC hydrogels without or with 0.67% of HA or GY785. From the top to the bottom: no staining, calcein AM dye (living cells in green), ethidium homodimer-1 dye (dead cells in red), alcian blue and hematoxylin/eosin/safranin-O staining of paraffin embedded hydrogels. Scale bar = 20 μ m



**Si-HPMC
(2)**

**Si-HPMC/HE800
(2/0.17)**

**Si-HPMC/HE800
(2/0.34)**

**Si-HPMC/HE800
(2/0.5)**

Figure 11: Optical images of C28/I2 cells cultured over 5 weeks in 3D within Si-HPMC hydrogels without or with HE800 at various concentrations. *Scale bar = 50 μ m*